



Science Arts & Métiers (SAM)

is an open access repository that collects the work of Arts et Métiers Institute of Technology researchers and makes it freely available over the web where possible.

This is an author-deposited version published in: <https://sam.ensam.eu>
Handle ID: <http://hdl.handle.net/10985/25281>

To cite this version :

Maya GEOFFROY, Pierre-Marc FRANÇOIS, Roman Hossein KHONSARI, Sébastien LAPORTE - Paediatric skull growth models: A systematic review of applications to normal skulls and craniosynostoses - Journal of Stomatology, Oral and Maxillofacial Surgery - Vol. 123, n°5, p.e533-e543 - 2022

Any correspondence concerning this service should be sent to the repository

Administrator : scienceouverte@ensam.eu



Review

Paediatric skull growth models: A systematic review of applications to normal skulls and craniosynostoses

Maya Geoffroy^{a,b,c,*}, Pierre-Marc François^c, Roman Hossein Khonsari^b, Sébastien Laporte^a

^a Arts et Métiers Institute of Technology, Université Paris Nord, IBHGC - Institut de Biomécanique Humaine Georges Charpak, HESAM Université, F-75013, Paris, France

^b Service de Chirurgie Maxillofaciale et Chirurgie Plastique, Hôpital Necker – Enfants Malades, Assistance Publique – Hôpitaux de Paris; Faculté de Médecine, Université de Paris; 149 Rue de Sévres, 75015 Paris, France

^c BONE 3D; 14 Rue Jean Antoine de Baïf, 75013 Paris, France

S U M M A R Y

Introduction: Craniosynostoses affect 1/2000 births and their incidence is currently increasing. Without surgery, craniosynostosis can lead to neurological issues due to restrained brain growth and social stigma due to abnormal head shapes. Understanding growth patterns is essential to develop surgical planning approaches and predict short- and long-term post-operative results. Here we provide a systematic review of normal and pathological cranial vault growth models.

Material and Methods: The systematic review of the literature identified descriptive and comprehensive skull growth models with the following criteria: full text articles dedicated to the skull vault of children under 2 years of age, without focus on molecular and cellular mechanisms. Models were analysed based on initial geometry, numerical method, age determination method and validation process.

Results: A total of 14 articles including 17 models was reviewed. Four descriptive models were assessed, including 3 models using statistical analyses and 1 based on deformational methods. Thirteen comprehensive models were assessed including 7 finite element models and 6 diffusion models. Results from the current literature showed that successful models combined analyses of cranial vault shape and suture bone formation. **Discussion:** Growth modelling is central when assessing craniofacial architecture in young patients and will be a key factor in the development of future customized treatment strategies. Recurrent technical difficulties were encountered by most authors when generalizing a specific craniosynostosis model to all types of craniosynostoses, when assessing the role of the brain and when attempting to relate the age with different stages of growth.

Keywords:

Pediatrics
Development and growth
Calvaria
Sutures
Craniosynostosis

1. Introduction

1.1. Background

Craniosynostoses (CS) are a group of rare diseases affecting 1/2000 to 1/2500 births per year [1], caused by the premature fusion of cranial sutures. In most cases, CS affect a single suture and are isolated conditions called non-syndromic craniosynostoses (NSCS). The origins of suture fusion are not well understood. Syndromic forms of CS also exist but are less common [2]. In these forms, multiple sutures are generally affected, extracranial anomalies can be reported, and genetic mechanisms are better deciphered.

NSCS incidence is currently on the rise, by 12.5% between 1997 and 2013 [3] without any known cause. NSCS are named according to the deformation resulting from the early fusion of one or more specific sutures: scaphocephaly results from early sagittal suture fusion (40 to 50% of all NSCS cases), trigonocephaly from early metopic fusion (3 to 27%) and plagiocephaly from early unilateral coronal fusion (13 to 16%). Multiple suture fusions lead to deformations such as brachycephaly and oxycephaly, and represent the remaining percentages [4].

Because of the interactions between skull and brain development [5], NSCS can potentially lead to cognitive impairment and vision loss due to intracranial hypertension [6]. The surgical management of NSCS is the current standard of care. Procedures aim to decrease intracranial pressure when needed and restore optimal forehead, orbital, and skull vault shapes [7].

Treatment schedules depend on the surgical technique and the craniosynostosis type. There is a current lack of consensus on the optimal age for surgery, especially for scaphocephaly [4,6]. A better

* Corresponding author.

E-mail addresses: maya.geoffroy@ensam.eu (M. Geoffroy), pierremarc.francois@bone3d.com (P.-M. François), roman.khonsari@aphp.fr (R.H. Khonsari), sebastien.laporte@ensam.eu (S. Laporte).

understanding of skull growth could contribute to solve this question. Furthermore, to improve the outcomes of these procedures and decrease the duration of surgical procedures, 3D surgery planning is slowly becoming standard in clinical practice. 3D planning still requires improvements, mostly in the field of growth predictions. In clear, successful planning relies on a close understanding of craniofacial growth [8].

Bone formation in the skull vault relies on two interacting mechanisms – suture growth and surface growth – which share a common driving force: brain expansion [9]. *Suture growth* is the deposition of bone on the margins of the sutures, and exponentially decreases from birth until 4 years of age [10]. Normal suture fusion takes place at different ages according to the anatomical localization: 67% of children have total fusion of the metopic suture at 7 months of age [11] while the coronal, sagittal and lambdoid start fusing in the adult life. *Surface growth* is the combination of resorption on the endocranial surface and deposition on the external surface, is also known as *drift* and leads to progressive thickening/thinning of the skull vault bones [12]. These conjoined mechanisms lead to the radial and axial translation of the vault bones compared to the base of the skull.

1.2. Study rationale

Taking into account suture and surface bone deposition when modelling skull vault growth is not sufficient. In fact, the correspondence between suture fusion and the resulting abnormal skull shape in NSCS is not as straightforward as generally admitted in the literature. The most commonly cited theory, Virchow's law, states that restricted growth perpendicular to the fused suture explains the final skull shape [13]. Nevertheless, trigonocephaly or oxycephaly are not easily explained by Virchow's law. A potential role of the skull base and its synchondroses in abnormal skull vault growth in NSCS has been postulated [9]. Other authors proposed mechanisms based on decreased growth potential around the fused suture, compensatory growth of all other sutures far from the fused suture and the dura mater distributing the forces abnormally [12,14]. In brief, the mechanisms leading to the abnormal shapes in NSCS still require investigation.

1.3. Study objective

The present study aimed to present a systematic review of the methods and results of all cranial vault growth models published in the literature to date. Both normal growth models and growth models for craniosynostoses have been analysed, as initial geometries could be similar and models for malformations required controls. We assessed models from the literature with two focuses: (1) type of model and (2) resulting skull geometries.

2. Material and methods

A detailed search was performed using four databases: Google Scholar, Science Direct, Semantic Scholar and PubMed. The following key words were used: model, growth, development, calvaria, skull, neurocranium, suture, craniosynostosis. Synonymous keywords (i.e. growth and development) were not searched together and all keywords were used independently and conjoined in the search. For instance, keywords 'growth model calvaria', 'growth model suture' and 'growth model calvaria suture' were screened in all 4 search engines. The 10 first results in order of 'best match' or regarding relevance were analysed.

The letters, reviews, abstracts, communications and context documents were excluded, as were the articles where the full text could not be found. Abstracts were read and the eligibility criteria enabled to find the topics applied (Fig. 1).

For this review, only numerical models based on human subjects aged 0–2 were selected. These criteria were used to ensure that the time period was consistent with the peaks of craniofacial growth. Only growth models applied to normal human skulls and human skulls affected by craniosynostosis were analysed. Primary ossification is a pre-natal phenomenon and was therefore not taken into account. Furthermore, biological models on microscopic scales were not considered. The last screening occurred on in December 2021, by a single reporter (first author MG)

Included models were analysed based on two categories: (1) descriptive and (2) comprehensive models. (1) *Descriptive models* used imaging to obtain actual geometries of subjects at different ages. The methods applied in these models were either statistical or based on deformations. (2) *Comprehensive models* used template geometries and applied mechanical laws to reproduce growth dynamics using either reaction-diffusion equations or Finite Element modeling (FEM). Comprehensive models allowed studying growth while assessing anatomy and material properties. These models aimed to reproduce the physiological behaviour of a growing skull and adapt to shape and/or constraints (for cases with early suture fusions). For both categories, the geometry of the input data, numerical method used and validation process were described.

The results of model assessment were finally analysed regarding potential clinical applications, both for controls and craniosynostoses.

3. Results

A total of 14 articles including 17 models were reviewed (Table 1). Four descriptive models were found (Table 2), including 3 models using statistical analyses [15–17] and 1 based on deformational methods [18]; amongst those, 3 used whole cranial vault geometry and 1 focused on sutures. Thirteen comprehensive models (Table 3) were found including 7 FEM [19–24] and 6 diffusion models [16,25–28]; amongst those, 4 were two-dimensional (2D) and 9 were three-dimensional (3D); amongst these 13 2D and 3D models, 7 focused on the whole cranial vault and 6 focused on sutures. Three suture models focused on suture interdigitation, 2 on suture ossification and 1 on both. Sixteen models analysed normal cranial vault growth and 6 studied growth of skulls affected by craniosynostosis.

3.1. Descriptive models

Descriptive models were analysed based on initial geometry, alignment process, landmarks positioning, numerical method, age determination method and validation process.

Descriptive models were based on actual geometries (Fig. 2). In three models, CT-scans of patients between 0 and 3 years of age were segmented [15,17,18] with either OsiriX (Pixmeo, Switzerland) [29] or 3D Slicer [30]. The scans were then used individually or grouped into mean models within specific age ranges: 8 scans for the age range 39–40 weeks and 11 scans for the age range 41–42 weeks enabled to develop 2 template models [18]. More unusual methods to extract geometries were used by another author [16] such as the replication of the suture shapes using high-resolution dental casting material and tracing of the sutures using Photoshop (Adobe Photoshop CS. (2004). Berkeley, CA: Peachpit Press). All descriptive models studying whole skulls considered them to be symmetrical along their sagittal axis.

Skulls were aligned using reference planes such as the mid-sagittal plane [17] and the Frankfurt plane [15] as well as anatomical landmarks such as the porion, basion [15], zygo-orbitale [15], and temporo-parietal suture [17]. Internal structures were also used to define the Talairach space [31] – characterised by the anterior commissure (AC) and the posterior commissure (PC) – and align the data

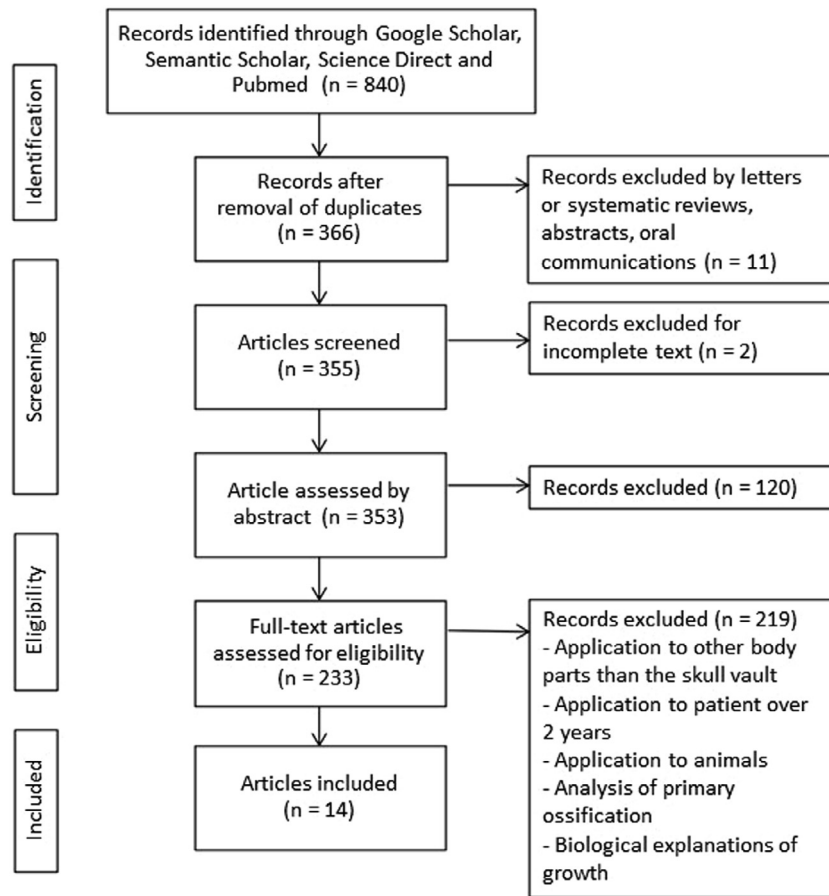


Fig. 1. PRISMA flow-chart. The PRISMA flowchart shows the sources reviewed, the number of articles screened and the articles included in the study.

[18]. Alignment could be avoided by using the Fourier transformation to analyse spatial frequency rather than space [16].

The positioning of landmarks on anatomical reference elements was used as a reproducible method for comparing geometries. These landmarks included suture-bone boundaries, suture intersections or semi-landmarks on bone surfaces derived from either or both types. Models had various amounts of landmarks placed between subjects depending on the extent of suture fusion (less suture-boundaries identifiable when sutures were fused) [17] and on the choice of their quantity - from 80 [15] to 92 [17] on new-born half-skulls.

Landmarks positioning was not necessary when Fourier transformation was used and when deformation rather than position was analysed [18].

Descriptive models were based on statistical methods such as Principal Component Analysis (PCA), a multivariate statistical procedure aiming to describe shapes and expressing them with eigenvectors accounting for the greatest variance. These methods were applied to landmarks, semi-landmarks, distances or complete meshes (of full skulls, cranial vault bones, or sutures) [15–17]. Descriptive models also included deformation models based on the mapping of

Table 1

Models included into the review, described by research group, model type, main method, ROI, dimension and scope and geometry.

Research group	Model type	Main method	ROI	Dimension	Scope
Zollikofer and Weissmann 2011 [16]	Descriptive	Statistical	Suture	2D	Normal
Li et al. 2015 [17]	Descriptive	Statistical	Vault	3D	Normal
Mercan, Hopper, and Maga 2020 [15]	Descriptive	Statistical	Vault	3D	Normal and NSCS
Mohtasebi et al. 2020 [18]	Descriptive	Deformation	Vault	3D	Normal
Jin et al. 2014 [20]	Comprehensive	FEM	Vault and brain	3D	Normal
Libby et al. 2017 [22]	Comprehensive	FEM	Vault	3D	Normal
Jalbert 2013 [19]	Comprehensive	FEM	Vault	3D	Normal and NSCS
Weickenmeier et al. 2017 [24]	Comprehensive	FEM	Vault	2D	Normal and NSCS
Weickenmeier et al. 2017 [24]	Comprehensive	FEM	Vault	3D	Normal and NSCS
J. Jin, Eagleson, and Ribaupierre 2018 [21]	Comprehensive	FEM	Vault	3D	Normal and NSCS
Malde et al. 2020 [23]	Comprehensive	FEM	Vault	3D	Post-operative scaphocephaly
Oota, Ono, and Miyazima 2006 [28]	Comprehensive	Diffusion	Suture	3D	Normal
Miura et al. 2009 [27]	Comprehensive	Diffusion	Suture	2D	Normal
Zollikofer and Weissmann 2011 [16]	Comprehensive	Diffusion	Suture	2D	Normal
Garzón-Alvarado, González, and Gutiérrez 2013 [26]	Comprehensive	Diffusion	Vault and suture	3D	Normal
Burgos-Flórez, Gavilán-Alfonso, and Garzón-Alvarado 2016 [25]	Comprehensive	Diffusion	Suture	2D	Normal
Burgos-Flórez, Gavilán-Alfonso, and Garzón-Alvarado 2016 [25]	Comprehensive	Diffusion	Vault	3D	Normal and NSCS

ROI: region of interest.

Table 2

Descriptive models, detailed by research group, aim, suture affected, ROI, dimension and type, data origin and model.

Research group	Aim	Suture affected	ROI	Dimension and type	Data
Zollikofer and Weissmann 2011 [16]	Study suture growth	NA	Sagittal sutures	2D PCA	Step length
Li et al. 2015 [17]	Develop statistical model	NA	Half-skulls with base and sutures	3D PCA	60 landmarks placed on 56 0–3 months-old half skulls
Mercan, Hopper, and Maga 2020 [15]	Develop statistical model	NA, S	Half-skulls with sutures	3D PCA	38 landmarks placed on 234 normal and 162 skulls with scaphocephaly half skulls of 0–6mo patients
Mohtasebi et al. 2020 [18]	Assess skull growth	NA	Full skulls and sutures	3D Deformation	2 CT templates developed from mean geometries from eight 39–40 week-olds and eleven 41–42 week-old new-borns.

NA: not affected (normal geometry); PCA: principal component analysis; ROI: region of interest; S: sagittal.

different skulls to a template skull. Deformation were computed between the two skulls when the studied geometries were mapped in the same manner [18]. The deformation field matrix was used to determine the differences in volume expansion, shrinkage, or areas with no volume change.

Model validation (Table 4) was performed by comparing skull vault shapes at different ages with cephalometric data such as length, width, height, circumference, cephalic index (CI), and intracranial volume from age-matched patients. One measurement was taken as reference to determine the link between the timeline of the simulation and experimental growth data. The age at each time point of the simulation could then be estimated and cephalometric data at corresponding ages were used to validate the model. The correspondence between simulation-time and growth-time determined for one simulation case could be re-used for other simulations. Models used either

the head circumference [17] from growth charts [32] or geometry modification distribution adjusted to age distribution [15] as reference elements to determine the ages at the different stages of the growth model.

The comparison methods for validation purposes were diverse: from 3D evaluation [17] to insufficient [16,18], or no validation process [15]. The 3D validation process consisted in analysing 3D distances between the actual and predicted landmarks placed on respectively 15 segmented CT-scans and on the skull resulting from the model [17]. Another possibility used in the literature [16] was a result comparison between a descriptive and a comprehensive model developed and discussed in the same article. Also, a group [18] analysed the head circumference, size of anterior and posterior fontanels as well as cranial bones, fontanels and sutures surface areas without quantitative comparison using clinical data.

Table 3

Comprehensive models, detailed by research group, aim, suture affected, ROI, dimension and type, data origin and model.

Research group	Aim	Suture affected	ROI	Dimension and type	Data
Jin et al. 2014 [20]	Hybrid brain and cranial vault growth model	NA	Full skull and brain	3D FEM	CT scan from a 21 days-old infant skull
Libby et al. 2017 [22]	Model of skull growth	NA	Full skull and brain	3D FEM	Mean model of 61 CT skulls between 273 and 294 days of age
Jalbert 2013 [19]	Model of skull growth	NA, UC, BC, Mini, Madv, S	Cranial vault with sutures	3D FEM	Ellipsoid cut through a basal plane of an 18 days-old skull
Weickenmeier et al. 2017 [24]	Models of skull growth	NA, UC, BC, M, L	Axial slice of the cranial vault and sutures	2D FEM	Contour of a new-born skull, MRI slice, at its widest transverse cross-section, scaled to a CI of 78.
Weickenmeier et al. 2017 [24]	Model of skull growth	NA, UC, BC, M, S, L	Cranial vault with sutures	3D FEM	Ellipsoid with a CI of 78, with 13 distinct regions
J. Jin, Eagleson, and Ribau-pierre 2018 [21]	Model of skull growth	NA, UC, M, S	Full skull with sutures	3D FEM	CT scan from a 21 days-old infant skull
Malde et al. 2020 [23]	Predict calvaria morphology	S	Full skull with sutures	3D FEM	CT scan from a 90 days-old infant, after surgery
Oota, Ono, and Miyazima 2006 [28]	Model of skull growth and suture fusion	NA	Sagittal suture	3D Diffusion	Rectangular walls separated by a uniform void, adjusted dimensions
Miura et al. 2009 [27]	Model of interdigitations	NA	Sagittal suture	2D Diffusion	Unknown periodic structure
Zollikofer and Weissmann 2011 [16]	Model of skull growth	NA	Sagittal suture	2D Diffusion	512 × 128 periodic lattice
Garzón-Alvarado, González, and Gutiérrez 2013 [26]	Model of ossification centres	NA	Full skull with sutures	3D Diffusion	Simplified prenatal skull with 32 mm length and 48 mm width
Burgos-Flórez, Gavilán-Alfonso, and Garzón-Alvarado 2016 [25]	Model of bone and suture formation	NA	Sagittal suture	2D Diffusion	Mesh, with 12 mm sutures, 5 mm sutures and 29 mm length
Burgos-Flórez, Gavilán-Alfonso, and Garzón-Alvarado 2016 [25]		NA	Complete skull with sutures	3D Diffusion	Simplified prenatal skull with 32 mm length and 48 mm width

BC: bicoronal; CI: cephalic index (biparietal diameter over the longest diameter from frontal bone to occipital bone i.e. skull width over length); CT: computed tomography; FEM: Finite element model; L: lambdoid; M: metopic; Mmi: metopic, mild model; Msev: metopic, severe model; NA: not affected (normal geometry); ROI: region of interest; S: sagittal, UC: unicoronal.

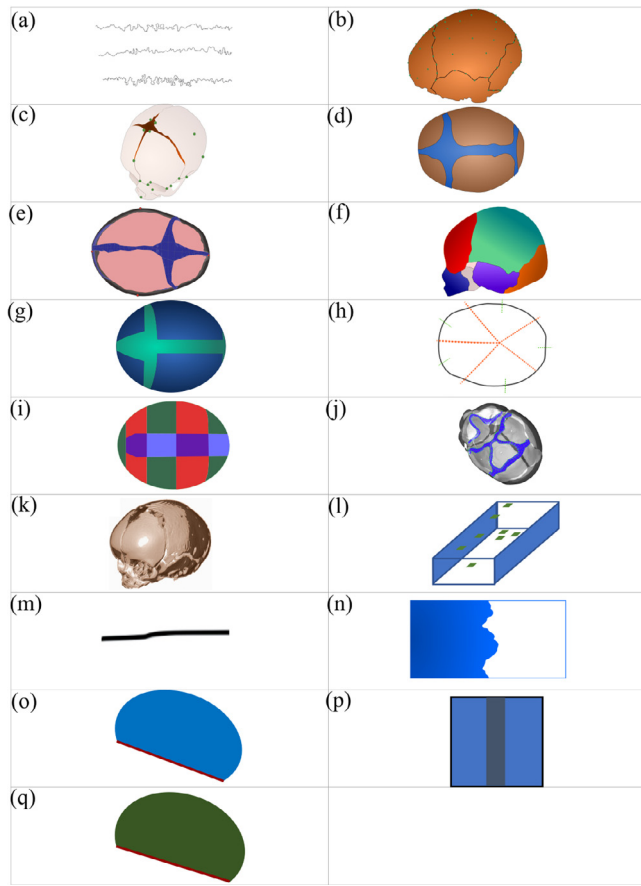


Fig. 2. Initial geometries for descriptive and comprehensive models (adapted from literature, area colour depending on the main method: white – statistical; dark grey – Deformation; blue – FEM; light grey – diffusion)(a) Sagittal sutures used for the PCA [16];(b) Half skull with landmarks used for the PCA[17]; (c) Complete skull with the landmarks and semi-landmarks[15]; (d) Probability map of suture patency and reconstruction for 41–42 weeks[18]; (e) 3D FEM of an infant skull (upper view)[20]; (f) 3D FEM of an infant skull (lateral view)[22]; (g) 3D FEM of an infant skull (upper view) [19]; (h) 2D transverse plane model[24]; (i) 3D FEM of an infant skull (antero-lateral view)[24]; (j) FEM of an infant skull (inferior view)[21]; (k) Follow-up geometry[23]; (l) 3D suture model[28]; (m) 2D suture model [27]; (n) 2D suture digitation bi-directional model, half model [16]; (o) Suture development model on a 3D vault[26]; (p) Suture digitation model[25]; (q) Suture development model on a cranial vault[25].

3.2. Comprehensive models

Comprehensive models were analysed using the initial geometry considered, element types used, material properties and boundary conditions, for normal growth models and skulls presenting with craniosynostoses. Age determination and validation process were also assessed.

The data were issued from very young infants in all models (from birth to 3 months of age). In three models, initial geometries originated from the skull of a single subject [20,21,23] segmented with Amira/Avizo (Thermo Fisher Scientific, Mass, USA). Other cases used a mean model [22], an ellipsoid scaled to a template subject [19,24–26], or simplified 2D or 3D sagittal suture models [16,25,27,28]. A simplification of the skull geometry was performed by ignoring the skull base in two cases [19,24].

Concerning 2D models, the cranial vault bones were modelled using beam elements [24] and sutures were modelled as constrained nodes. A 2D model used a lattice structure [16]. For 3D models, triangular shell [25,26], quadratic shell [19], quadratic tetrahedral [22] or hexahedral elements, and eight-node linear brick elements [24] were used to model the vault and sutures, sometimes combining two types of elements [19–21].

Material properties had various definitions according to the models (Table 5) with Young moduli ranging from 300 MPa [19] to non-deformable [20,21]. For the sutures, the Young modulus ranged from 10 MPa [19] to 200 MPa [20,21]. Reference data used mostly originated from experimental data for bone and suture [10,33]. The rigidification of bone with age [33] did not fully explain the Young modulus chosen by the researchers. Only one model adapted material properties to simulate stiffening of the skull with growth: suture properties were increased by 200 MPa in seven intervals and the metopic suture was also fused at 8.5 months [23].

Bone growth could be modelled as a homogeneous expansion along principal axis of beams for a 2D growth model [24], without considering the internal structures. Another possibility was to model growth as a result of the primary expansion of the brain, through a thermal linear expansion of internal structures [22,23]. For these models, a basal element of the skull was constrained, and the bony elements expand secondarily to intracranial volume expansion. Besides, two models [19,21] applied forces and pressures on the inner surface of the cranial vault. The internal pressure used – 0.001 MPa [19] – was consistent with age-matched normal ICP values (18 days).

Table 4

Model validation described by research group, compared ages, reference measurement, measurements for validation.

Research group	Compared ages	Reference measurement	Measurements for validation
Zollikofer and Weissmann 2011 [16]	NS	Descriptive model results	NS
Li et al. 2015 [17]	NS	Head circumference	NS
Mercan, Hopper, and Maga 2020 [15]	NS	NS	NS
Mohtasebi et al. 2020 [18]	NS	NS	NS
Jin et al. 2014 [20]	NS	NS	Evolution of CI variations with age
Libby et al. 2017 [22]	0–12 months-old	ICV	Width, length, circumference, 3D shape
Jalbert 2013 [19]	NS	NS	NS
Weickenmeier et al. 2017 - 2D model [24]	NS	Normal cephalic index	Average pathological cephalic index over the compared ages
Weickenmeier et al. 2017 - 3D model [24]	NS	Normal cephalic index	Average pathological cephalic index over the compared ages
Jin, Eagleson, and Ribapierre 2018 [21]	0–12 months-old	Normal circumference growth rate (%)	NS
Malde et al. 2020 [23]	29 months-old	ICV from the same patient at a different age	Cephalic index, length, width, height, 2D cross-sections and 3D distance colour maps
Garzón-Alvarado, González, and Gutiérrez 2013 [26]	11 months-old	Evolution of molecule concentration over time	NS
Burgos-Flórez, Gavilán-Alfonso, and Garzón-Alvarado 2016 [25]	NS	Evolution of molecule concentration over time	NS
Burgos-Flórez, Gavilán-Alfonso, and Garzón-Alvarado 2016 [25]	NS	Time evolution of molecule concentration	NS

ICV: intracranial volume; NS: not specified.

Table 5

Finite Element Models, described by research group, anatomical elements included, mesh type, material properties, number of elements and loads applied for modelling growth.

Research group	Age of the initial geometry	Anatomical elements	Mesh	Materials	Number of elements	Loads applied for modelling growth
Jin et al. 2014 [20]	3 weeks old	Bone	Rigid surface	$\rho = 2070 \text{ kg/m}^3$ $\rho = 1130 \text{ kg/m}^3$, $E = 200 \text{ MPa}$, $\nu = 0.28$	NS	Outwards pressure on the volumetric brain model
		Suture	Hexahedral		NS	
		Bone-suture interface	Spring		NS	
Libby et al. 2017 [22]	1 months old	Brain	Tetrahedral	$\rho = 1040 \text{ kg/m}^3$ $E = 1 \text{ MPa}$, $\nu = 0.48$ $E = 3000 \text{ MPa}$, $\nu = 0.3$ $E = 30 \text{ MPa}$, $\nu = 0.3$ $E = 100 \text{ MPa}$, $\nu = 0.48$	NS	Isotropic linear expansion of the ICV
		Bone	Tetrahedral		1040,000	
		Sutures	Elastic solid			
Jalbert 2013 [19]	18 days	ICV	Tetrahedral	$E = 300 \text{ MPa}$, $\nu = 0.28$ $E = 10 \text{ MPa}$, $\nu = 0.28$ $E = 150 \text{ MPa}$, $\nu = 0.28$	13,919	Pressure on the internal table of 0.001 MPa
		Bone	Hexahedral			
		Sutures	Hexahedral			
Weickenmeier et al. 2017 - 2D model [24]		Basal plane	Shell	$E = 150 \text{ MPa}$, $\nu = 0.28$ E dependant on age, $\nu = 0.28$	194	Volumetric growth, deposition, remodelling applied on the bone Constrained nodes for the sutures
		Bone	Beam			
		Sutures	Nodes moving along suture lines			
Weickenmeier et al. 2017 - 3D model [24]	Newborn	Bone	Hexahedral	E dependant on age, $\nu = 0.28$	13 regions	Volumetric growth, deposition, remodelling for the bone Strain-driven linear elastic expansion applied unidirectionally for the sutures and bidirectionally for the fontanelles
		Suture	Hexahedral			
		Fontanelles	Hexahedral			
Jin, Eagleson, and Ribaut-pierre 2018 [21]	3 weeks	Bone	Rigid surface	$\rho = 2070 \text{ kg/m}^3$ $\rho = 1130 \text{ kg/m}^3$, $E = 200 \text{ MPa}$, $\nu = 0.28$ $\rho = 2070 \text{ kg/m}^3$ $E = 3000 \text{ MPa}$, $\nu = 0.3$ $E = 30 \text{ MPa}$, $\nu = 0.3$ $E = 100 \text{ MPa}$, $\nu = 0.48$	NS	Outward customizable force on the inner surface nodes Constrained basal plane
		Suture	Hexahedral		NS	
		Basal plane	Shell		NS	
Malde et al. 2020 [23]	3 months	Bone	Quadratic tetrahedral	$E = 3000 \text{ MPa}$, $\nu = 0.3$ $E = 30 \text{ MPa}$, $\nu = 0.3$ $E = 100 \text{ MPa}$, $\nu = 0.48$	1600,000	Isotropic linear expansion of the ICV
		Suture and craniotomies				
		ICV			200,000	

E: Young Modulus, ν : Poisson ratio, ρ : density.

Only one research group modelled the brain as an independent structure, and applied an expanding pressure (of unknown value) [20]. A comprehensive modelling of three growth phenomena (bone deposition, surface remodelling and brain growth) was also performed [24]. Different growth mechanisms were analysed in this 3D model: (1) the metopic and sagittal sutures were involved in transversal expansion, (2) coronal and lambdoid sagittal in lengthening, and (3) fontanelles for bidirectional growth. One suture model [16] modelled growth through a strain-driven deformational process, where the elastic surface stretching was dependant on the growth. Boundary conditions used to model growth were diverse and considered brain growth at various extents.

All the models analysed the cranial vault shape using cephalometric data such as cranial vault head, width, height, circumference, intracranial volume and cephalic index [20,21]. Furthermore, other data were analysed such as the 3D shapes [22,23], node displacement [24], tension along the sutures [20,21], stress distribution [20], and Von Mises constraints [19].

Concerning suture models, the formation of interdigitation and the suture width were modelled using reaction-diffusion equations [27]. One model reproduced the characteristic shape of interdigitations with a minimal amount of parameters [16]. Another method consisted of modelling sutural growth as a random accumulation of bone material inside the suture area [28]. Diffusion models

were also applied on ellipsoids representing the cranial vault with suture growth from ossification centres [25,26]. All groups working on sutures stated the importance of the dura-mater and its role in transmitting strain resulting from the primary expansion of the brain, leading to the development of the sutures. Two models [16,27] considered this element by including strain dissipators and underlying molecular mechanisms that could model the dura mater role in growth.

All NSCS growth models were based on an initial 'normal' skull shape (Fig. 2). Accordingly, the boundary conditions of comprehensive models needed to be modified to account for the cranial vault shape modifications due to suture fusion. Two groups [19,21] chose to model closed sutures as bone, as recommended in the literature [34]. Degree of suture fusion in NSCS models was introduced [19] by defining severe, intermediate, and mild cases of trigonocephaly respectively corresponding to 0%, 30% and 50% open sutures. In all cases, the constraints applied to closed sutures were identical to the ones applied to bony elements. Post-operative cranial growth of sagittal craniosynostosis was also modelled [23]; craniotomies were modelled as sutures, contact areas were modelled as bonded and the Young modulus of the sutures was increased with the simulation time-step. In addition, normal metopic suture fusion was implemented at 8.5 months. Suture models mostly did not model the fusion process, although an evaluation of the impact of the

concentration of one molecular factor (TGF- β 3) involved in craniosynostoses was performed [25].

As for descriptive models, a link between age and shape needed to be determined. The determination of the relationship between simulation-time and growth-time was defined thanks to the head circumference rate of normal infants and applied to infants with craniosynostosis [21]. Suture closure clearly correlated with age. However, the analysis of the suture closure timing was limited to qualitative analysis [25,26] and performing an age-matched quantitative analysis was not proposed.

Validation processes were limited to qualitative methods for some groups [19,20] but all other groups used quantitative methods. For simulated skull vault shapes, validation was performed at different ages in terms of length, width, height, CI, and intracranial volume from aged-matched patients [21,22]. For the post-operative model assessment, a distance plot between the result of the growth model and the geometry of the same patient was performed [23]. Two groups [20,24] were also able to avoid specifying the age of the subjects for validation by using a ratio such as the CI. Suture interdigitation did not correlate with age ($R = 0.51$) [16] and these models thus only analysed shapes.

3.3. Application to normal growth

Normal growth models are summarised in Fig. 3. One descriptive model showed that PC1 (first principal component) was correlated with age ($R^2 = 0.68$) and explained 35% of the variations of the control cohort, enabling the development of a growth model [15]. The authors established that the growth of the frontal and parietal bones was faster than the growth of the fontanelle, leading to its closure. Furthermore, fontanelle closure would primarily be caused by parietal bone growth rather than by frontal bone growth. The modelling of growth was performed up to 179 days. Interestingly, another descriptive model focused on the first 21 days of growth showed that an increase in size of fontanelle took place before its shrinkage [18], linked to the expansion of the brain.

One 2D model [24] reported a globally homogenous normal growth of the skull quantitatively evaluated through the displacement of all nodes of the model. 3D descriptive and comprehensive models further found that the skull tended to be spheroid; analyses of width, height, length, anterior fontanelle size, intracranial volume, and CI showed an increase with age for normal skulls [18,21,24]. Models either found almost linear [20,21] or logarithmic growth [22]. Skull height seemed to increase before length and width [20]. The stresses and constraints at the sutures were more important at the anterior fontanelle and at the face / cranial vault interface [19–21], most likely because it was modelled as rigid. However, one model [24] showed more displacement of the nodes at the superior and lateral areas of the frontal bone, without further quantitative analysis.

Regarding sutures at a macroscopic level, one group [17] provided data, from new-born to 3 years-old patients, on the speed and schedule of suture closure as well as on bone thickness. Bone thickness analysis concluded that the frontal and parietal bones were thinner than the occipital bone. Age, head circumference and landmark placement were significant predictors of suture width and skull thickness.

On a smaller scale, the interdigitation pattern of sutures could be analysed. 2D models found that fractal dimension and the amplitude of the interdigitations increased with simulation time, similarly to clinical observations [16,27]. One study [16] established parameters applied to normal suture interdigitation which only correlated with the first three PCs (26%) of the descriptive model developed by the same research group. Thus, the rest of the PCs were attributed to inter-individual variations. 3D modelling of the sutures that considered the impact of the dura mater was also developed [28]. The results were analysed for the internal, middle, and external sections

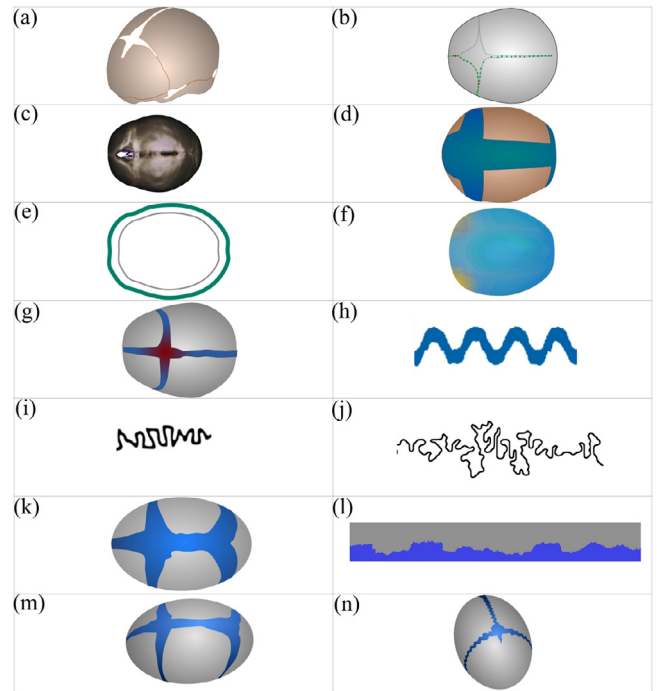


Fig. 3. Normal growth models results, adapted from literature (area colour depending on the main method: white – statistical; dark grey – Deformation; blue – FEM; light grey – diffusion) (a) Statistical normal growth model, at 1 year old[17]; (b) Normal growth model at 179 days[15]; (c) Deformation model, with colours corresponding to the Jacobian matrix value[18]; (d) Normal growth model[19]; (e) 2D section of normal skull growth; colourmap corresponding to skull displacement field [24]; (f) 3D upper view of normal skull growth; colourmap corresponding to skull displacement field [24]; (g) Normal growth model[21]; (h) Example for the middle section of the suture [28]; (i) Interdigitation results with circle sprouting pattern [27]; (j) Example of suture interdigitation obtained with the following parameters: surface tension on time step of 500 for a Laplacian growth, no multiplier applied [16]; (k) 3D suture model, upper view of the calvaria at 2 months[26]; (l) Developmental model at 8 months[25]; (m) Suture interdigitation result at 15 months[25]; (n) Combined models at 14 months [25].

of a suture considered in a sagittal section plane. Other suture models aimed to analyse growth starting from ossification centres to fusion, on an ellipsoid [25,26]. These models combined suture interdigitation and suture development from ossification centres (but not brain growth impacting the macroscopic cranial vault size) [25]. The models reproduced suture width and bone shapes, matching clinical data.

Validation processes were generally not sufficient (Table 4). Concerning suture interdigitation models, only qualitative comparison to physiological sutural shape was performed. One model [16] validated choices of parameters by developing variants. Local changes of suture interdigitation around the parietal foramina were obtained. Concerning cranial vault models, the evolution of the CI was used for validation compared to clinical data, without much success for one group [20]. Only one group [22] performed a quantitative validation by comparing the in vivo scans in terms of circumference, length, width, ICV, and 3D shape, for boys and girls, to the FEM results of patients up to 11 or 12 months of age. Only the head circumference of girls showed to be significantly different between FEM and clinical data. The differences on the vault were mainly underpredictions by the model (face, frontal bone, orbital and temporal region) although some areas of overpredictions existed (parietal, occipital and fontanelles). All other models [15,17–19,21,24–28] did not propose a proper validation process.

These studies showed that although the normal skull seems to grow linearly outwards, analysis on a smaller scale needed to be considered. In fact, the local growth of the frontal and parietal bones explained better the evolution of the fontanelle, where stresses were

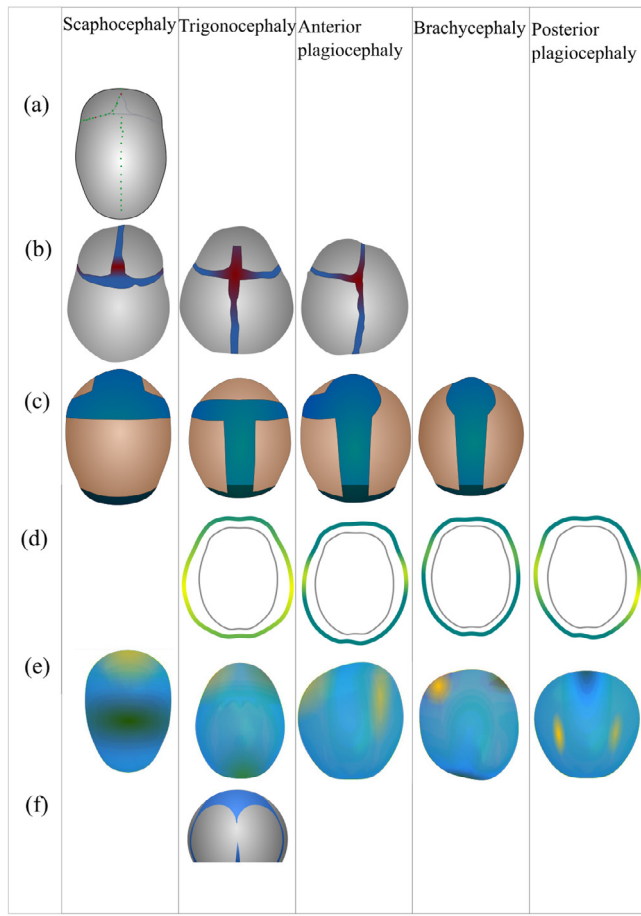


Fig. 4. Craniosynostosis model results, according to the type(s) analysed (adapted from literature) (a) Upper view of the scaphocephaly growth model at different ages [15]; (b) Upper view of the advanced age [19]; (c) 3D model of craniosynostosis, colour-map referring to the normalized displacement [24]; (d) 2D model of craniosynostosis, colourmap referring to the normalized displacement [24] (e) Growth models of craniosynostosis [21]; (f) Parameter changes on the metopic suture [25].

important. Furthermore, suture development from ossification sites and interdigitations were important factors in growth. Model validation also needed to be generalised to all studies and quantitative validation with age references needed to be applied.

3.4. Application to craniosynostosis

All craniosynostosis growth models are summarised in Fig. 4. A descriptive growth model for scaphocephaly [15] used PCA (principal component analysis) and found that PC1 accounted for 30% of the variability, corresponded morphologically to an increase in skull size and was correlated with age ($R^2=0.59$). Compared to normal growth, the analysis demonstrated a restriction in the medio-lateral direction for the parietal bones, and in the supero-inferior direction.

Comprehensive models attempted to qualitatively reproduce existing shapes and determine which factors influenced the outcomes of the simulation in normal children and children with NSCS. However, modelled shapes did not always match clinical observations [4,6]. Scaphocephaly was specifically well modelled, with a satisfactory rendering of skull elongation. For anterior plagiocephaly, the characteristic contralateral flattening and ipsilateral bulging above the orbit and frontal bone was obtained [19,24]. The contralateral compensatory growth was however not obtained when bone was modelled as solid [20,21]. Likewise, the results concerning trigonocephaly were varied: the triangular shape was globally obtained in one model [21] whereas others did not obtain the compensatory

posterior widening [19,24]. Metopic ridges and hypotelorism, associated with trigonocephaly, were never obtained, most likely because the face up to the orbits was modelled as solid and the fused sutures were often modelled as bone [34], leading to a fixed forehead geometry [19,21,24]. The modelling of brachycephaly and posterior plagiocephaly were similar to anterior plagiocephalies and mostly satisfactory.

Only one research group studied post-operative results [23] and proved feasibility on a single subject of a novel way of modelling sutures evolution with age. The model showed a good correspondence with an in vivo subject at 29 months of age, on the sagittal, coronal, and transverse cross-sections. The 3D shape comparison showed a maximum overprediction of 10.86 mm and underprediction of 22.30 mm.

Concerning suture models, the increase of the coefficients promoting differentiation of mesenchymal tissue was assumed to lead to suture fusion, thus mimicking NSCS [27]. Yet, no results supporting this hypothesis were presented. A study [25] based the modelling of NSCS on the modification of the concentration of TGF- β 3 to determine the areas of patency or fusion of sutures. This model was applied to the premature fusion of the metopic suture at 3.5 months of age, most likely because physiological fusion of sutures is uncommon (10–33%) before 3 months of age [11]. The qualitative results were discussed without quantitative comparison and without considering the compensatory and restricted growth of the rest of the skull linked to the metopic suture fusion.

Validation was conducted through quantitative comparisons. The CI values found by the group that analysed both 2D and 3D growth [24] were in accordance with clinical values reported in literature, without further analysis of distribution. The use of this ratio enabled comparison without relation to patient age. More generally, researchers solely performed qualitative comparisons of shapes obtained from models [19,21,24–26]. Only one model [23] validated FEM using the same subject as the one used for the input geometry. The distance plot between the two geometries showed a maximum of 22 mm underprediction and 10 mm overprediction (of unknown location) and a 0.03 underprediction of the CI and thus confirmed the modelling choices.

4. Discussion

The present study aimed to present a review of the methods and results of all cranial vault growth models published in the literature to date. Models mainly varied based on the modelling method used (descriptive or comprehensive), the geometries considered, the inclusion or exclusion of brain growth and the validation method. The assessment of 17 different models suggests that successful approaches should combine analyses of the cranial vault shape and of the suture bone formation.

4.1. Article selection

The number of articles found was limited due to a general difficulty for researchers to find data on skull growth in children. Articles only focused on morphological changes without interpolating or extrapolating the data to obtain a model were not included. Models based on animal data were excluded. Paediatric growth models were especially difficult to build and validate as few subjects benefited from multiple image acquisitions to be used as reference and validation data, as repeated irradiation from CT-scans has to be avoided as much as possible in young patients. Perspectives in this field rely on the development of efficient, mostly AI-based, segmentation methods for specific MRI sequences dedicated to bone imaging, such as the black bone sequence [35].

4.2. Shape of the cranial vault

Descriptive models used non-simplified patient geometries. They contributed to the understanding of the skull vault, base, and fontanelle growth. For PCA, landmarks and semi-landmarks were manually positioned. This step limited the analysis of the surface of the bony plates and thus could bias the analysis of the overall shape. In fact, landmarks were placed on the suture edges [15] and only one model used 24 landmarks placed on the skull surfaces [17]. Models should use larger numbers of landmarks and semi-landmarks over the bone surfaces to better predict the overall shape of the skull.

Several elements impacting the shape of the cranial vault were not extensively analysed in the current literature. Clinical observations show that due to growth, normal sutures tend to drift towards the opposite side relative to the fused suture. However, one model [24] constrained suture node movements along the suture lines. Furthermore, fontanelles are clearly impacted in NSCS [15] but only one model [24] distinguished the anterior and posterior fontanelle regions and defined specific constraints. Moreover, the fact that the severity of suture fusion may impact the shape of the cranial vault needs to be confirmed and eventually considered, for instance using three different degrees of metopic suture fusion [19]. Suture drift in NSCS, fontanelle involvement and degree of suture fusion may have an impact on the geometry of the skull and should thus be better assessed in future models.

4.3. Considerations on adjacent structures

All models included the skull vault bones and the sutures with CT-derived or simplified geometries. A global consensus states that brain growth is the primary factor causing cranial vault expansion [36]. Yet the brain was only fully modelled once [20] and generally considered as a joined structure with the ICV [22,23] or only taken into account through its interaction with the skull vault bones using forces or pressure [19,21]. However, intracranial pressure could be different in each type of craniosynostoses, with regional variations, although there is no consensus on the subject [36]: brain growth modelling in NSCS still requires further theoretical investigations.

For paediatric growth models, it is important to consider bone anisotropy, density and thickness differences: the three layers of skull vault bones (inner table, medulla, outer table) are formed around 4 years of age [37]. However, all cranial vault models except one [24] considered the bone to be a uniform and isotropic element. Furthermore, bone thickness was considered homogenous over the vault surface for 2 models [15,19] even though the parietal bone is thinner than the occipital bone, which could have an impact on its behaviour when loaded [38].

Including bone remodelling into the simulations led to satisfactory results in one case [24]. In fact, this phenomenon is responsible for bone thickening and the pneumatization of the frontal sinus, located on the lower aspect of the frontal bone [39]. Both these phenomena vary with and/or could be influenced by NSCS. This leads to propose that including bone remodelling in normal and craniosynostosis models is a promising perspective.

Obtaining paediatric bones for mechanical testing is complex because of the difficulty of harvesting large samples in size and volume for research purposes. Nonetheless, many factors like bone stiffening with age, and fibre orientation and localisation should be included in the models: [33,40] in fact, the Young modulus of bone increases with age, by a factor of 50 from birth to 2 years of age [10]. Furthermore, collagen fibre orientation perpendicular to the long axis of the specimen leads to stiffer bones than a parallel orientation [40], and parietal bone is stiffer than, for example, occipital bone [33]. Other elements potentially interesting to integrate in further models are less consensual, such as inter-individual differences, ethnic background, the impact of sample conservation procedures [33],

the impact of testing rate and the use of estimations from animal model data.

Approaches including extensive data on sutures may lead to a more inclusive understanding of growth. In fact, current models solely focused on the sagittal suture, neglecting the coronal and lambdoid sutures. However, the development of sagittal sutures cannot be generalised to all sutures: non-midline sutures develop by overlapping their borders while midline sutures (metopic and sagittal) develop front to front [12,37]. Furthermore, the location of the ossification centres on the calvaria influence suture development [26]. Further modelling efforts are required to consider the morphological diversity of sutures and not only rely on data from the sagittal suture.

Fused sutures are considered equivalent to bone [34]. However, there is a significant difference between the Young modulus of parietal bone and fused sutures. For instance, parietal bone suture tested on its convex surface had a Young modulus of 1398+/-599 MPa while the fused suture tested on the same side were at 941+/-588 MPa [19].

The complexity of the sutures (that is, the degree of interdigitations) does not strongly correlate with age but bone formation at the contact surfaces of primary ossification sites does. Descriptive models [15,17] analysed the width of the sutures at different ages as well as the age of the metopic suture fusion. However, all but 4 comprehensive models [21,23,25,26] used simulation time to describe their results. Comprehensive models should attempt to model bone formation with respect to age as a reference for future models with premature fusion of sutures.

The growth of the skull base and of the cranial vault covary [41] and skull base growth could affect skull length [37]. However, current comprehensive models could not include the skull base as synchondrosis do not behave as sutures [12].

Concerning the face, trigonocephaly patients often present with hypotelorism, which is corrected during surgery [7]. However, the face is generally not modelled [19,24-26], or modelled as a single non-deformable area [21,22]. However, the degree of fusion of the fronto-sphenoidal suture impacts the orbital shape [42]. Craniosynostosis models should thus also include the upper orbital rim.

4.4. Validation methods

The validation processes were limited by the fact that many cephalometric data were not independent, such as brain cavity volume, circumference, length, and width. In consequence, if the reference element used to determine the age of the patient at the advanced stage of the model was biased (for example by gender), the measurements used for the validation were equally biased. For instance, males were found to have bigger heads than females but this factor was not taken into account when determining the age of subjects. To limit this bias, the weight rather than the age can be used [40]. Only one comprehensive model took gender into consideration for the analysis [22], with unavoidable computational costs.

Furthermore, the use of cephalometric data to validate cranial growth models applied to craniosynostosis could lead to inadequate results. In particular, using the growth rate of head circumference to establish the link between growth-time and simulation-time [20,21] can lead to wrong computations of patient age. In fact, head circumference is often lower for trigonocephaly and greater for scaphocephaly [43] even though this point is rarely quantitatively assessed. Furthermore, ICV is reduced in many multiple suture CS and is sometimes diminished for trigonocephaly at one month of age but normalises around 6 months of age. This led to the conclusion that 2D measurements and ICV are not fit to assess global shape in craniosynostoses. To tackle these issues, 3D shape analysis could greatly improve the assessment of growth models, but was only performed to a limited extent [17,22,23].

4.5. Alternative methods for growth modelling

Of note, many other models have been developed, but not explicitly for the understanding of normal growth or growth applied to craniosynostosis patients. In particular, other statistical methods than PCA exist. In particular, Principal Component Regression (PCR) and Partial Least Square Regression methods could have been used to develop growth models. Both methods aim to reduce dimensions and could be used to express shapes depending on covariances.

Also, general mathematical models for the initial stages of suture formation [44], morphology analysis [45], specific models on mice were found in the literature with considerations on growth after suture fusion [46] or models applied strictly to suture fibrous tissue growth [47]. These comprehensive models were not included into the current review.

5. Perspectives

Current studies tend to introduce landmark-free approaches by implementing template mesh morphing, projections, or non-rigid iterative closest point algorithms. For instance, warping from adult skulls to corresponding infant skulls [48], or the application of PCA on all nodes of a skull thanks to non-rigid iterative closest point (NICP) registration can be performed. Moreover, PCA can also be applied to deformation vectors which are independent from landmarks, as performed in cases with trigonocephaly [49] and scaphocephaly [45]. PC1 here again captured head size which could have led to a 3D growth model of pre-operative skulls, but also of post-operative results, which were rarely analysed using 3D methods. These different methods could easily be adapted to develop growth models.

The brain was never completely and anatomically modelled although it plays a central role in the growth of the cranial vault. A descriptive model [50] of the endocranium (approximating the brain) for different age confirmed that it influenced skull growth. A PCA model analysed brain morphology [5] and showed that the brain had an abnormal shape in non-syndromic unicoronal craniosynostosis compared to controls. This PCA analysis indicated that the deformation was present from birth and did not increase with age. Moreover, brain regions have different growth rates and exert non-uniform pressures on cranial bones – and this could be used to enrich craniosynostosis growth models [41]. Descriptive and comprehensive models should include the brain and analyse its geometry to improve the clinical relevance of cranial vault growth models.

Several other internal structures of the skull could also be included in further models. The dura mater and the falx cerebri may have a mecano-transduction roles by transmitting forces induced by brain growth to the inner surface of the skull vault, all along the midline and on the lesser wings of the sphenoid, the petrous temporal crests, and the posterior edge of the foramen magnum [12,37].

Declaration of Competing Interest

The authors declare that there is no conflict of interest.

Acknowledgements

The study was supported by BONE 3D.

References

- [1] Mathijssen IMJ. Guideline for care of patients with the diagnoses of craniosynostosis: working group on Craniosynostosis. *J Craniofac Surg* 2015;26:1735–807.
- [2] Wilkie AOM, Johnson D, Wall SA. Clinical genetics of Craniosynostosis. *Clin Genet Craniosynostosis* 2017;29:622–8.
- [3] Kolar JC. An epidemiological study of nonsyndromal craniosynostoses. *J Craniofac Surg* 2011;22:47–9.
- [4] Bennis Y, Wolber A, Vinchon M, Belkhou A, Duquennoy-Martinot V, Guerreschi P. Les craniosténoses non syndromiques. *Ann Chir Plast Esthet* 2016;61:389–407.
- [5] Aldridge K, Kane AA, Marsh JL, Panchal J, Boyadjiev SA, Yan P, et al. Brain morphology in nonsyndromic unicoronal craniosynostosis. *Anat Rec - Part A Discov Mol Cell Evol Biol* 2005;285:690–8.
- [6] Buchanan E, Xue Y, Xue A, Olshinka A, Lam S. Multidisciplinary care of craniosynostosis. *J Multidiscip Healthc* 2017;10:263–70.
- [7] Arnaud E, Marchac D, Renier D. Le traitement des craniosténoses : indications et techniques. *Neurochirurgie* 2006;52:264–91.
- [8] Andrew TW, Baylan J, Mittermiller PA, Cheng H, Johns DN, Edwards MSB, et al. Virtual surgical planning decreases operative time for isolated single suture and multi-suture craniosynostosis repair. *Plast Reconstr Surg - Glob Open* 2018;6:1–7.
- [9] Moss ML. Functional anatomy of cranial synostosis. *Childs Brain* 1975;1:22–33.
- [10] Henderson JH, Longaker MT, Carter DR. Sutural bone deposition rate and strain magnitude during cranial development. *Bone* 2004;34:271–80.
- [11] Vu HL, Panchal J, Parker EE, Levine NS, Francel P. The timing of physiologic closure of the metopic suture: a review of 159 patients using reconstructed 3D CT scans of the craniofacial region. *J Craniofac Surg* 2001;12:527–32.
- [12] Flaherty K, Singh N, Richtsmeier JT. Understanding craniosynostosis as a growth disorder. *Wiley Interdiscip Rev Dev Biol* 2016;5:429–59.
- [13] Virchow R. Über den Kretinismus, namentlich in Franken, und über pathologische Schädelformen. *Verhandlungen der Phys Gesellschaft Würzburg* 1851;2:230–56.
- [14] Delashaw JB, Persing JA, Broadus WC, Jane JA. Cranial vault growth in craniosynostosis. *J Neurosurg* 1989;70:159–65.
- [15] Mercan E, Hopper RA, Maga AM. Cranial growth in isolated sagittal craniosynostosis compared with normal growth in the first 6 months of age. *J Anat* 2020;236:105–16.
- [16] Zollikofer CPE, Weissmann JD. A bidirectional interface growth model for cranial interosseous suture morphogenesis. *J Anat* 2011;219:100–14.
- [17] Li Z, Park B, Liu W, Zhang J, Reed M, Rupp J, et al. A statistical skull geometry model for children 0–3 years old 2015;10:1–13.
- [18] Mohtasebi M, Bayat M, Ghadimi S, Moghaddam HA, Wallois F, Abrishami Moghaddam H, et al. Modeling of neonatal skull development using computed tomography images. *Irbm* 2020;1:1–9.
- [19] Fl Jalbert. *Mecano-biologie de la croissance crânienne: application aux craniosténoses*. Université de Toulouse; 2013.
- [20] Jin J, Shahbazi S, Lloyd J, Fels S, de Ribaupierre S, Eagleson R. Hybrid simulation of brain–skull growth. *Simulation* 2014;90:3–10.
- [21] Jin J, Eagleson R, Ribaupierre S. Skull development simulation model for craniosynostosis surgery planning. *Biol Eng Med* 2018;3:1–8.
- [22] Libby J, Marghoub A, Johnson D, Khonsari RH, Fagan MJ, Moazen M. Modeling human skull growth: a validated computational model. *J R Soc Interface* 2017;14.
- [23] Malde O, Cross C, Lim CL, Marghoub A, Cunningham ML, Hopper RA, et al. Predicting calvarial morphology in sagittal craniosynostosis. *Sci Rep* 2020;10:1–8.
- [24] Weickenmeier J, Fischer C, Carter D, Kuhl E, Goriely A. Dimensional, geometrical, and physical constraints in skull growth. *Phys Rev Lett* 2017;118:1–5.
- [25] Burgos-Flórez FJ, Gavilán-Alfonso ME, DA Garzón-Alvarado. Flat bones and sutures formation in the human cranial vault during prenatal development and infancy: a computational model. *J Theor Biol* 2016;393:127–44.
- [26] Garzón-Alvarado DA, González A, Gutiérrez ML. Growth of the flat bones of the membranous neurocranium: a computational model. *Comput Methods Programs Biomed* 2013;112:655–64.
- [27] Miura T, Perlyn CA, Kinboshi M, Ogihara N, Kobayashi-Miura M, Morriss-Kay GM, et al. Mechanism of skull suture maintenance and interdigitation. *J Anat* 2009;215:642–55.
- [28] Oota Y, Ono K, Miyazima S. 3D Modeling for sagittal suture. *Phys A Stat Mech its Appl* 2006;359:538–46.
- [29] Rosset A, Spadola L, Ratib O. OsiriX: an open-source software for navigating in multidimensional DICOM images. *J Digit Imaging* 2004;17:205–16.
- [30] Fedorov A, Beichel R, Kalpathy-Cramer J, Finet J, Fillion-Robin JC, Pujol S, et al. 3D Slicer as an image computing platform for the quantitative imaging network. *Magn Reson Imaging* 2012 Nov 1;30:1323–41.
- [31] Talairach J, Tournoux P. *Co-Planar stereotaxic atlas of the human brain*. New York: Thieme Medical Publishers, Inc.; 1988. p. 132..
- [32] Kuczmarski RJ, Ogden C, Guo SS, Grummer-Strawn L, Flegal K, Mei Z. CDC growth charts for the United States: methods and development. *Vital health stat. Vital Heal Stat* 11 2000;1.
- [33] Coats B, Margulies SS. Material properties of human infant skull and suture at high rates. *J Neurotrauma* 2006;23:1222–32.
- [34] Margulies SS, Thibault KL. Infant skull and suture properties: measurements and implications for mechanisms of pediatric brain injury. *J Biomech Eng* 2000;122:364–71.
- [35] Eley KA, Delso G. Automated segmentation of the craniofacial skeleton with “black bone” magnetic resonance imaging. *J Craniofac Surg* 2020;31:1015–7.
- [36] Persing JA. Considerations in the Treatment of Craniosynostosis 2008:1–11.
- [37] Jin SW, Sim KB, Kim SD. Development and growth of the normal cranial vault: an embryologic review. *J Korean Neurosurg Soc* 2016;59:192–6.
- [38] Chamrad J, Marcia P, Bora L, Marcián P, Borák L, Marcia P, et al. On the level of computational model of a human skull: a comparative study. *Appl Comput Mech* 2018;12:5–16.
- [39] Nikolova S, Toneva D, Georgiev I, Lazarov N. Relation between metopic suture persistence and frontal sinus development. *Intech*; 2018.
- [40] Kriewall TJ. Structural, mechanical, and material properties of fetal cranial bone. *Am J Obstet Gynecol* 1982;143:707–14.

- [41] Barbeito-Andrés J, Bonfili N, Nogué JM, Bernal V, Gonzalez PN. Modeling the effect of brain growth on cranial bones using finite-element analysis and geometric morphometrics. *Surg Radiol Anat* 2020;42:741–8.
- [42] Nagasao T, Miyamoto J, Uchikawa Y, Tamaki T, Yamada A, Kaneko T, et al. A bio-mechanical study on the effect of premature fusion of the frontosphenoidal suture on orbit asymmetry in unilateral coronal synostosis. *Cleft Palate Craniofac J* 2010;47:82–91.
- [43] Persing JA. MOC-PS(SM) CME article: management considerations in the treatment of craniosynostosis. *Plast Reconstr Surg* 2008;121:1–11.
- [44] Khonsari RH, Olivier J, Vigneaux P, Sanchez S, Tafforeau P, Ahlberg PE, et al. A mathematical model for mechanotransduction at the early steps of suture formation. *Proc R Soc B Biol Sci* 2013;280.
- [45] Heutinck P, Knoops P, Rodriguez-Florez N, Biffi B, Breakey W, James G, et al. Statistical shape modelling for the analysis of head shape variations. *J cranio-maxillo-facial Surg* 2021.
- [46] Lee C, Richtsmeier JT, Kraft RH. A computational analysis of bone formation in the cranial vault using a coupled reaction-diffusion-strain model. *J Mech Med Biol* 2017;17:1–18.
- [47] Lottering N, Alston CL, Barry MD, MacGregor DM, Gregory LS. Temporal mapping of the closure of the anterior fontanelle and contiguous sutures using computed tomography, in silico models of modern infants. *J Anat* 2020;237:379–90.
- [48] Lapeer RJA, Prager RW. 3D shape recovery of a newborn skull using thin-plate splines. *Comput Med Imaging Graph* 2000;24:193–204.
- [49] Rodriguez-Florez N, Bruse JL, Borghi A, Vercruysse H, Ong J, James G, et al. Statistical shape modelling to aid surgical planning: associations between surgical parameters and head shapes following spring-assisted cranioplasty. *Int J Comput Assist Radiol Surg* 2017;12:1739–49.
- [50] Neubauer S, Gunz P, Hublin JJ. The pattern of endocranial ontogenetic shape changes in humans. *J Anat* 2009;215:240–55.